Electronic Supplementary Material (ESI) for Physical Chemistry Chemical Physics


# The silver-oxygen system in catalysis: New insights by ambient pressure X-ray photoemission spectroscopy

## -Supporting information-

***1 – Carbon Removal***

Under 0.25mbar of $O_2$ and below 130 °C, the silver surface is covered with carbonates ($Ag_2CO_3$) and hydrocarbons arising either from residual gases inside the chamber or from contact with ambient (for the powder spectra that could not be cleaned in situ by Ar sputtering). The top spectrum in figure S1-a shows the C 1s core level for a fresh (i.e. untreated) silver foil measured under $O_2$ atmosphere at room temperature. The main peak at 284.3 eV is assigned to hydrocarbons (CHx) while the long asymmetric tail to high binding energy and the additional feature at 287 eV indicate the presence of many oxygen functionalized hydrocarbons and silver carbonate (287.7 eV). This assignment is confirmed by the broad peak around 531 eV in the O1s spectra (top spectra in figure S1b). The tail at high binding energies is most likely related to adsorbed $H_2O$ and OH. As the temperature is raised to 130-150 °C under $O_2$ atmosphere, firstly the hydrocarbons and then the carbonates gradually vanish until the silver surface is finally free of carbon after 10 min (bottom spectra in figure S1-a).

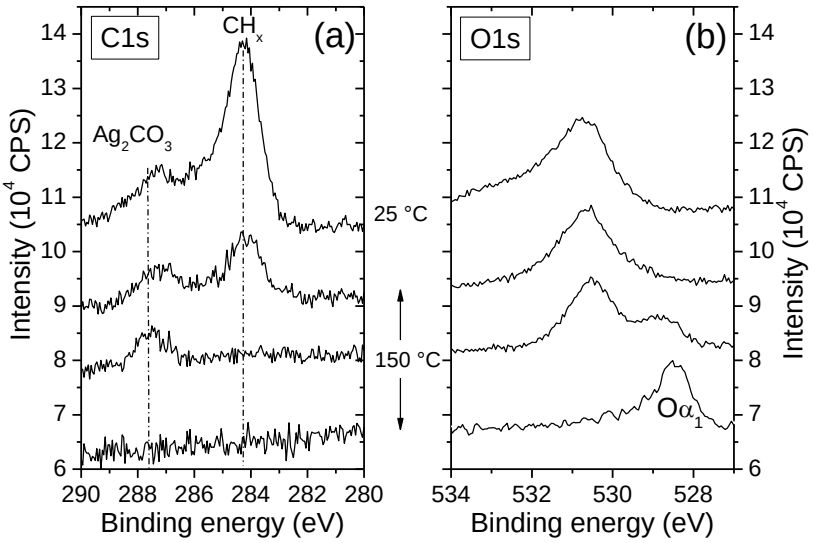


Figure S1. (a) C1s and (b) O 1s spectra of fresh silver foil following the temperature ramp from 25 to 150 °C.

***2 – fitting procedure and additional spectra – separation of* Oα3 and Oβ at 150-230C**

The O1s spectra were fitted with a set of 6 components with constrained peak positions and widths given in table S1.

Table S1. Fitting parameters for the O1s spectra

| component | BE (eV) | FWHM (eV)[a] |
|---|---|---|
| $O\alpha_1$ | 528.0-528.6 | 0.8-1.1 |
| $O\alpha_2$ | 529.0-529.3 | 0.9-1.1 |
| $O\gamma$ | 529.3-529.8 | 0.9-1.1 |
| $O\alpha_3$ | 530.0-530.6 | 0.9-1.1 |
| $O\beta$ | 530.7-531.3 | 1.0-1.2 |
| $SiO_2$ | 531.5-532.5 | 1.2-1.5 |

Figure S.2 provides additional data to support the separation of the feature at 530-531 eV into two components assigned as the electrophilic Oα3 species and the sub-surface Oβ. The same set of spectra was fitted considering only 1 peak (Figure S.2a) or 2 peaks (Figure S.2b).

Both models provide mathematically equivalent solutions for the fitting, as indicated by the average goodness of fit for all spectra that is only 2.5% better for the case of 2 peaks. This is a result of the small BE separation of the Oα3 and Oβ components (0.45-60 eV) relative to the FWHM (1.0-1.2).

However more insights can be obtained comparing the BE and FWHM for both cases. It is visible that the Opeak shifts broadens considerably, while less variations are present for the case of Oα3 and Oβ. This quantitatively represented in the histograms in figure S.2-c,d. It can be seen that narrower distributions of BE and FWHM are obtained when the feature is split into Oα3 and Oβ. Moreover, the obtained FHWM and the fluctuations in BE are more comparable to the other species Oα1 and Oα2.

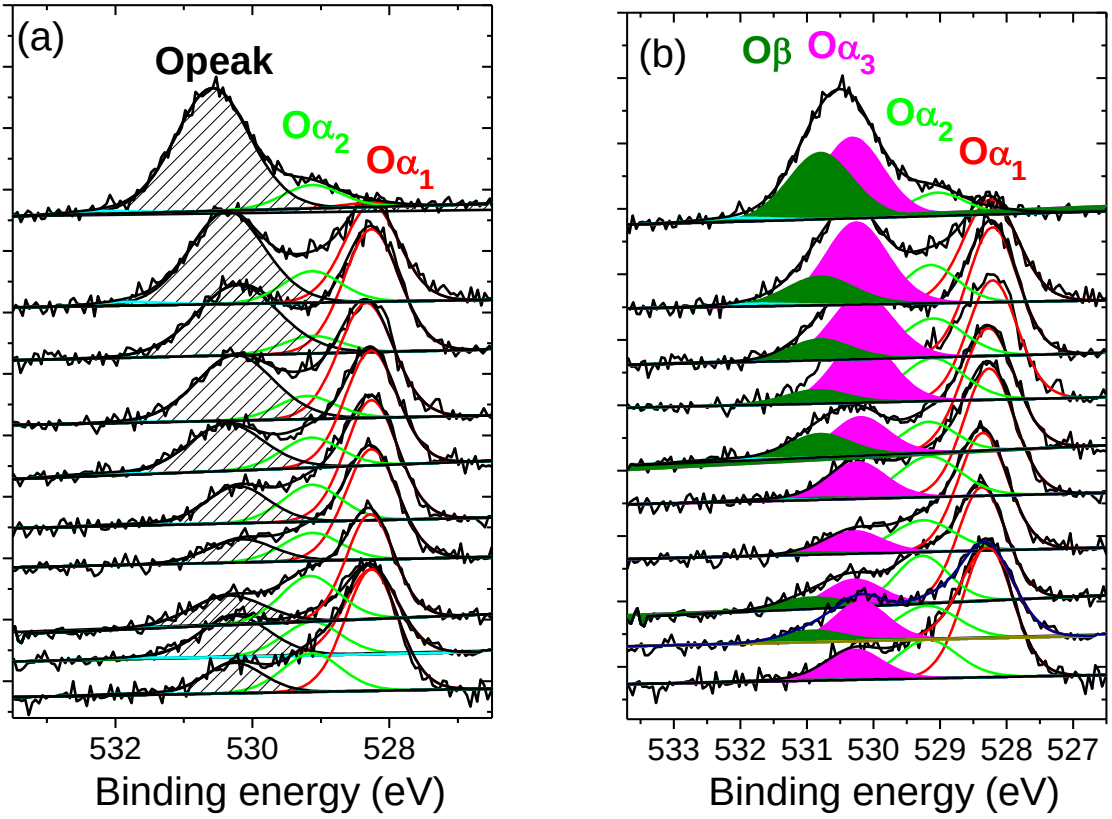


same BE axis annotation/scaling

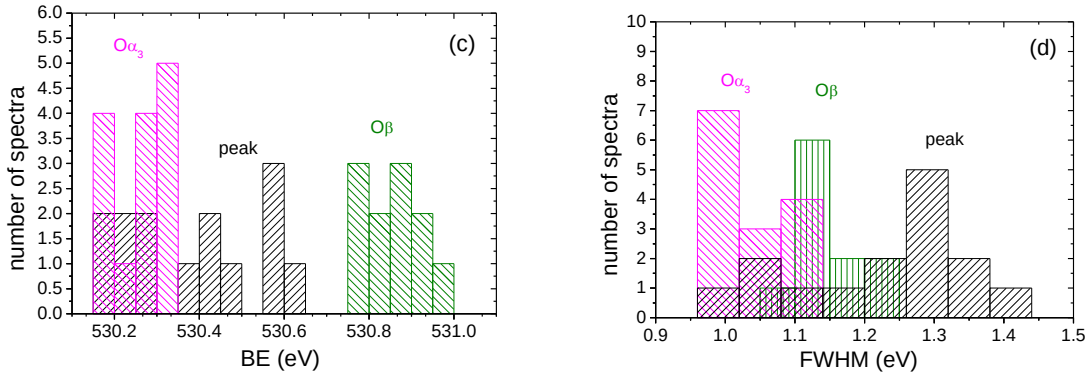


Figure S.2 – O1s Spectra for Ag(110) at different conditions. (a) Fitted using only one component for the 530-531 eV feature (Opeak). (b) same spectra fitted with two components (Oα3 and Oβ). (c) BE histograms. (d) FWHM histogram.

***3 - Si contamination***

Figure S.3 below shows the SEM characterization of an Ag foil with severe Si contamination. The foil was kept at 0.5 mbar $O_2$ at 500C for 72 h. As can be seen, the Si is segregated into 3D particles instead of wetting the Ag surface even in these areas of very high Si concentration.

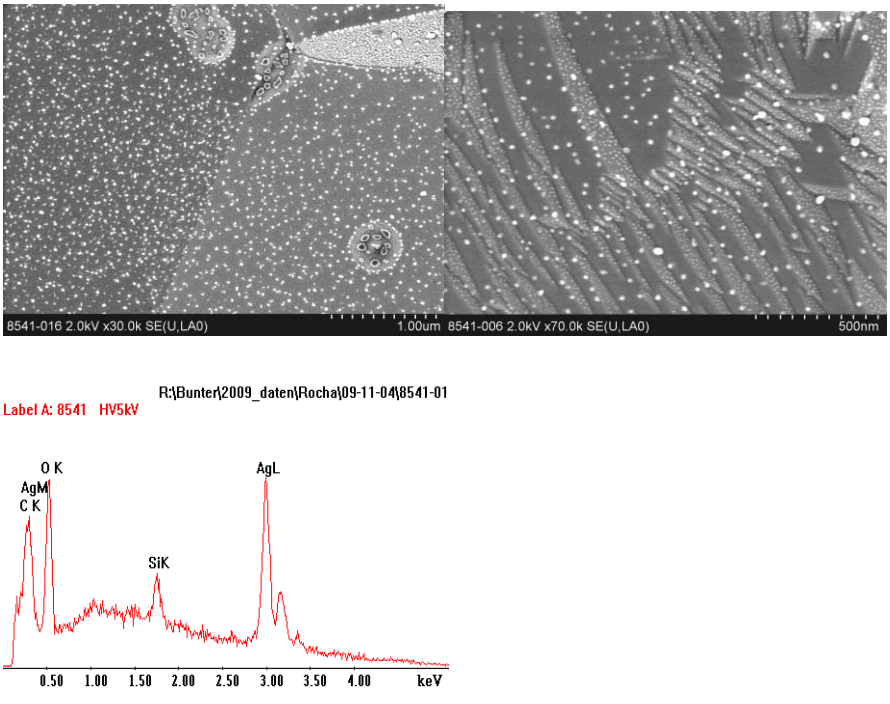


Figure S.3 – Ag foil not sputtered after exposed to O2 at 0.5 mbar at 500 C for 48 h. (a-b) secondary electrons SEM images. (c) EDX spectra showing the Si peak.

The Si2p signal that would be obtained by conventional lab source XPS measurements can be estimated by using theoretical cross sections and inelastic mean free paths shown in table S2. When the photon energy is changed from 350 eV (our case) to 1253.6 eV (Mg Kalpha), the cross section ratio Si2p/Ag4s ratio at 350 reduces from 9 to 1.6. Moreover considering that Si is on the Ag surface the change in IMFP from 6 to 16 A, causes a reduction by a factor of 2 in the Si/Ag signal ratio.

Table S2. Cross sectiction (σ) and inelastic mean free path for Si 2p and Ag 4s at photon energies 350 ev and 1253.6 eV.

| Element/transition | σ@350 (Mb) | σ@1253.6(Mb) | IMFP @350 (A) | IMFP @1253.6 (A) |
|---|---|---|---|---|
| Ag 4s | 0.1057 | 0.01211 | 6.4 | 16.3 |
| Si 2p | 0.9655 | 0.01914 | | |

Hence an overall decrease of a factor of approximately 11 is expected for the signal ratio of Si2p/Ag 4s. This is illustrated in figure S.4. With a survey spectra with hν=800 eV the Si2p is within the noise level (a-b). Figure S4c shows the Si 2p spectra measured with 350 eV photon energy where the Ag 4s and Si 2p peaks are clearly distinguishable. The small red curve is the Si2p peak attenuated by a factor of 11, as it would be expected for measurements with 1253.6 eV Mg Ka radiation. As can be seen, the Si 2p peak is slightly higher than the tail of the Ag4s and would be hardly visible considering the noise.

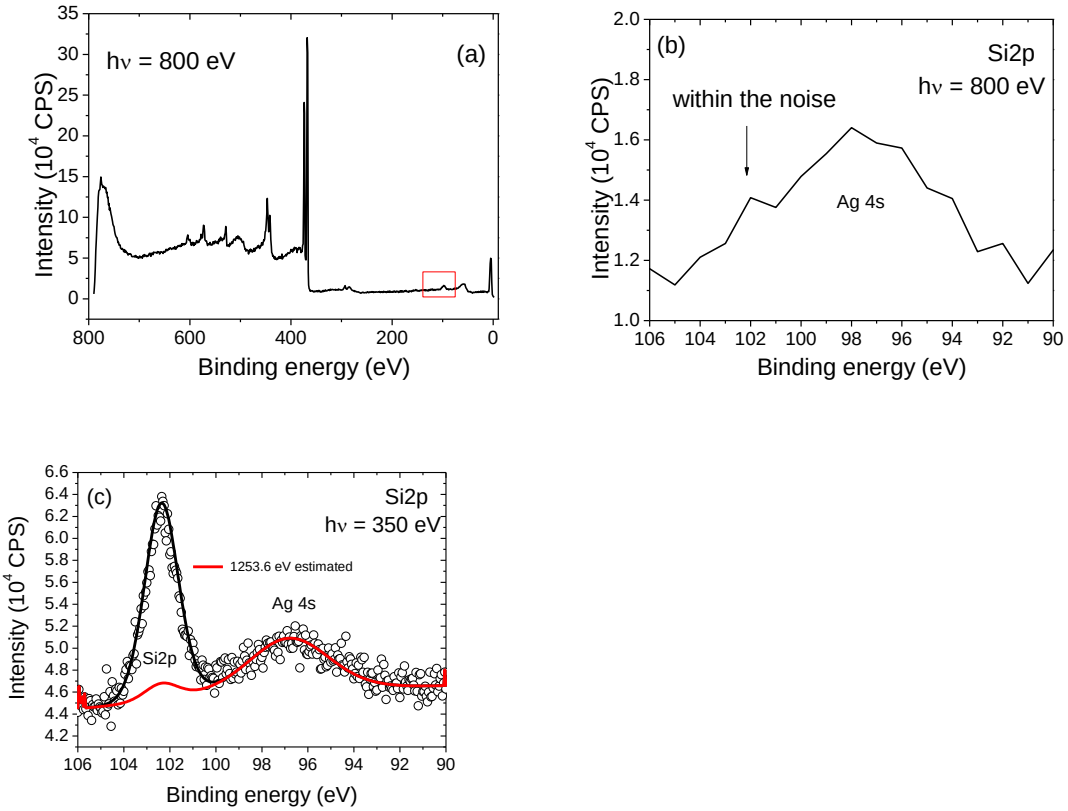


Figure S4. Ag foil under 0.2 mbar O2 and 500 C. (a) survey spectra with 800 eV photon energy and 1 eV step width. (b) zoom of the Si 2p area from survey with 800 eV photon energy. (c) Si 2p measured with 350 eV photon energy

### *4- The influence of Cl on the O species*

As shown in figure S.5 the presence of Cl in the Ag surface changes the distribution of oxygen species. Initially at Cl low concentrations, mostly the low BE species O$\alpha$1 and O$\alpha$2 are reduced ( blue, green, red spectra). At higher Cl concentrations, the higher BE species O$\alpha$3 is also reduced (black).

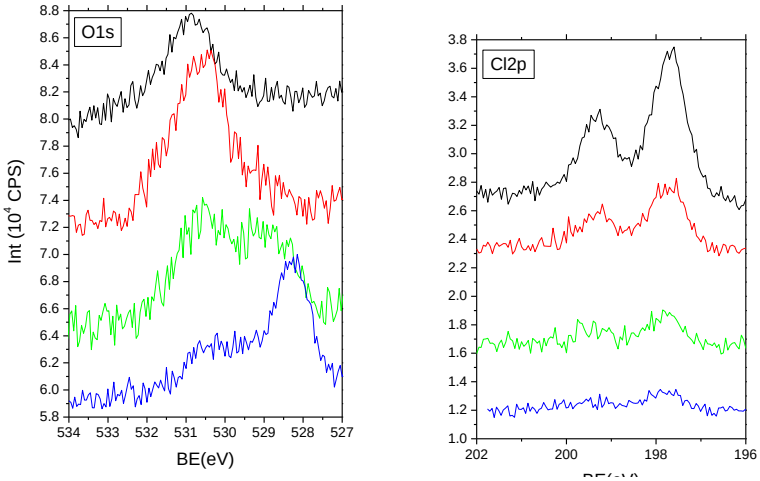


Figure S.5 – Consecutive O1s (a) and Cl2p (b) measured for the Ag(111) under $O_2$ at 200 C for which considerable segregation/deposition of Cl to the Ag surface was observed. The time difference between the spectra is 30 min.

## *5 - Calculation of $Ag^+$ O correlation*

The correlation of the amounts of Ag+ and the different O species was calculated by solving a linear system in which the concentration of different Oxygen species determined by XPS (O$\alpha$1, O$\alpha$2, O$\alpha$3, O$\beta$) are the coefficients, the unknowns (X1, X2, X3, X4) are the desired correlation factors and the Ag+ concentrations are the constants.

$$O\alpha_1 * X1 + O\alpha_2 * X2 + O\alpha_3 * X3 + O\beta * X4 + O\gamma * X5 - Ag = 0$$

For the case of the species at 150 to 230 C, the concentration of the O species and corresponding $Ag^+$ were calculated for a total of 25 pairs of O1s and Ag3d spectra and a linear system was constructed. The following system was solved using Mathematica software by minimization of a merit function constructed by the sum of the squares of each equation, with the constraint that the unknowns should be greater or equal to zero.

```
Minimize[{
  (0*X1 + 7.4*X2 +  12.6*X3 - 19.3)^2 +
  (0.1*X1 +  6.1*X2 +  9.6*X3 -  15.6)^2 +
  (0.3*X1 +  7*X2 +  25.6*X3 -  18)^2 +
  (0.2*X1 +  5.4*X2 +  4.6*X3 -  15.4)^2 +
  (0.3*X1 +  4.8*X2 +  5.4*X3 -  14)^2 +
  (0.2*X1 +  8.3*X2 +  17.4*X3 -  20.4)^2 +
  (1.1*X1 +  4.8*X2 +  4.2*X3 -  11.2)^2 +
  (0*X1 +  7.8*X2 +  21.6*X3 -  16)^2 +
  (5.6*X1 +  3.2*X2 +  3.5*X3 -  35.7)^2 +
  (4.8*X1 +  3.1*X2 +  2.1*X3 -  31.9)^2 +
  (0*X1 +  6.8*X2 +  8.8*X3 -  16.1)^2 +
  (0.2*X1 +  3.9*X2 +  5.8*X3 -  9.4)^2 +
  (0*X1 +  2.8*X2 +  5.3*X3 -  7)^2 +
  (2.3*X1 +  4.9*X2 +  11*X3 -  22.7)^2 +
  (1*X1 +  4.5*X2 +  5.3*X3 -  14.2)^2 +
  (0.2*X1 +  2.8*X2 +  8.5*X3 -  6.4)^2 +
  (4.2*X1 +  5.9*X2 +  5.3*X3 -  32.4)^2 +
  (0*X1 +  3.2*X2 +  5.8*X3 -  8.8)^2 +
  (1.6*X1 +  4.1*X2 +  12.9*X3 -  19.1)^2 +
```

```
125     (0.9*X1 + 1.8*X2 + 9.9*X3 - 9.3)^2 +
126     (1.9*X1 + 8.4*X2 + 13.9*X3 - 26.2)^2 +
127     (2.1*X1 + 6.8*X2 + 9.7*X3 - 25.7)^2 +
128     (5.6*X1 + 4*X2 + 3.2*X3 - 32.9)^2 +
129       (4.5*X1 +  5.5*X2 +  5.6*X3 -  33.1)^2,
130   X1 >= 0, X2 >= 0, X3 >= 0}, {X1, X2, X3}]
131   The solution of this system is
132   {73.0241, {X1→4.70536, X2→2.319, X3→0.0456375}}
133
```

### *6 - Valence band spectra*

In order to confirm the assignment of the features in the VB to oxygen, measurements with different photon energies were performed. As shown in figure S.6-a, when the photon energy is changed from 500 eV to 190 eV, the cross section for the O2p level increase relative to both the Ag5s and Ag4d, which causes an enhacement of the oxygen related features in the VB as illustrated in figures S.6-b,c for the case of Oγ and Oβ. The cross section ratio σ(O2p)/ σ (Ag4d) increases by a factor of 10 while the ratio σ(O2p)/ σ (Ag4s) increases by a factor of 6.

The pure gas phase spectra (solid out of x-ray beam) is included to show that the changes in the d and sp regions cannot be assigned to contributions from the gas phase molecular oxygen.

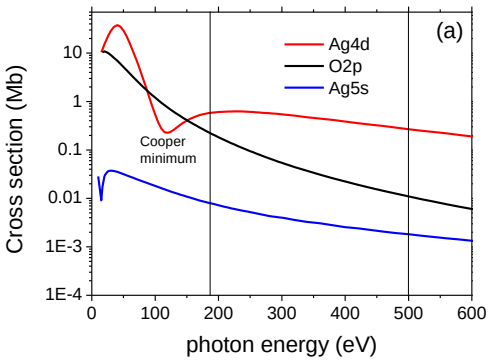


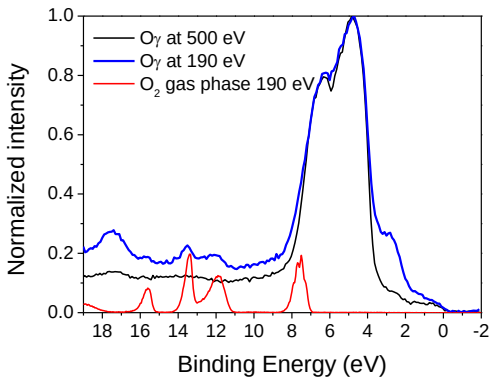


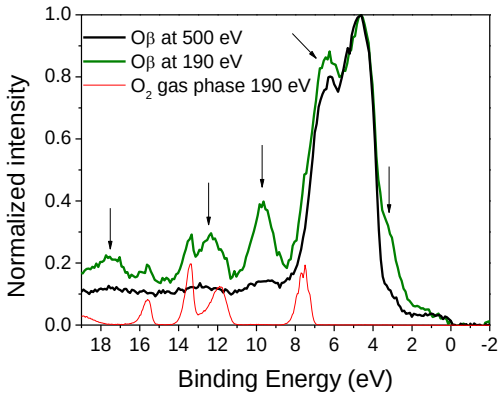

Figure S.6 – (a)Theoretical cross sections calculated by Yeh and Lindau for Ag4d, O2p and Ag5s []. VB spectra at 190 eV and 500 eV for Oγ (b) and Oβ (c). $O_2$ gas phase VBspectra is included for comparison.

***7 - Depth Profile***

The depth distribution of O species on Ag was probed by energy dependent XPS. By selecting different photon energies the O 1s and Ag 3d levels were measured using photoelectrons with different kinetic energy, which carry information from different depths. Three different well defined states were characterized where one of oxygen species is dominant. The preparation conditions are summarized in the table S3:

Table S3: Preparation conditions of well defined states for depth profile experiments

| Dominant species | Material | Temperature | Time |
|---|---|---|---|
| $O\alpha_1$ | Ag(111) | 150 C | 2 h |
| Oβ | Ag foil | 400 C | 6 h |
| Oγ | Ag foil | 500 C | 12 h |

O 1s and Ag 3d spectra were measured with different photon energies in order to have spectra with 230, 400, 600 and 900 eV kinetic energy. The O1s spectra at 230 eV kinetic energy are presented in figure S7-a. As can be seen not only the binding energy of the changes but also the total amount of oxygen. Figure S7-b shows the ratio of O and Ag atomic concentration obtained from the XPS quantification for the three states as function of the kinetic energy of the photoelectrons. In order to give an estimate of the average information depth at each kinetic energy, the corresponding inelastic mean free path is given in the top axis [see ref S1].

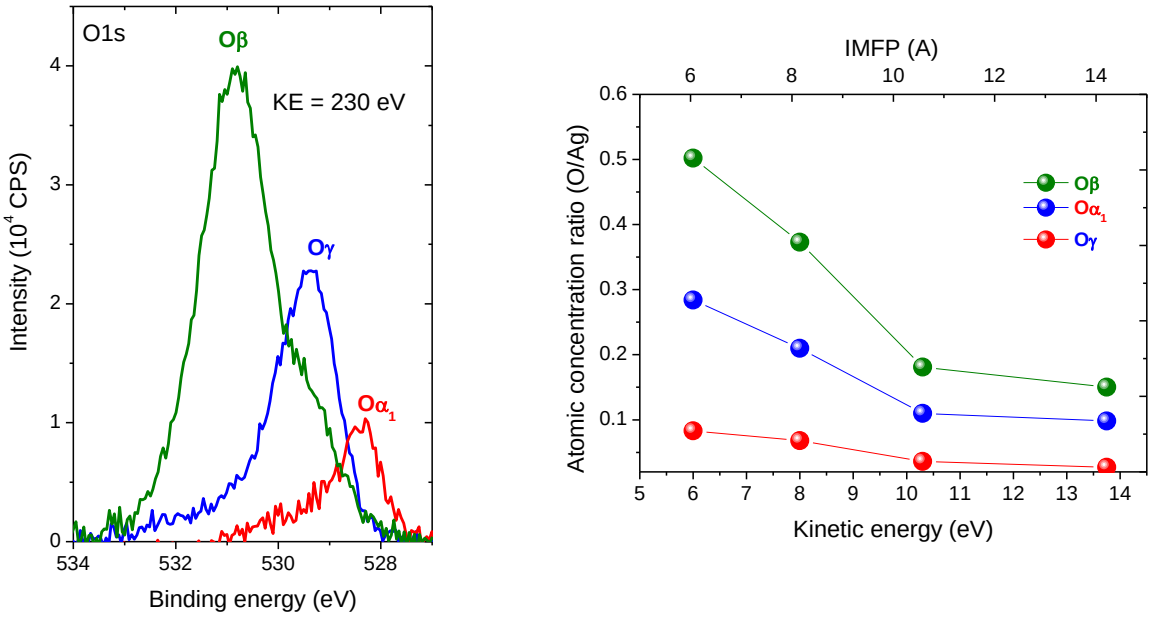


Figure S7. (a) O1s spectra at 230 eV kinetic energy for three different states of Ag samples. (b) Atomic concentration ratio O/Ag as function of the photoelectron kinetic energy.

The three different states present a large differences in the total amount of oxygen. The Oβ state has 6.2 times more oxygen that the state $O\alpha_1$. However the depth profile is nearly the same. The similarities of the three depth profiles can be better visualized in the normalized curves presented in figure S8. As can be seen the amount of oxygen drops to 30 % of the initial values as the kinetic energy is increased from 230 to 900 eV in all the cases.

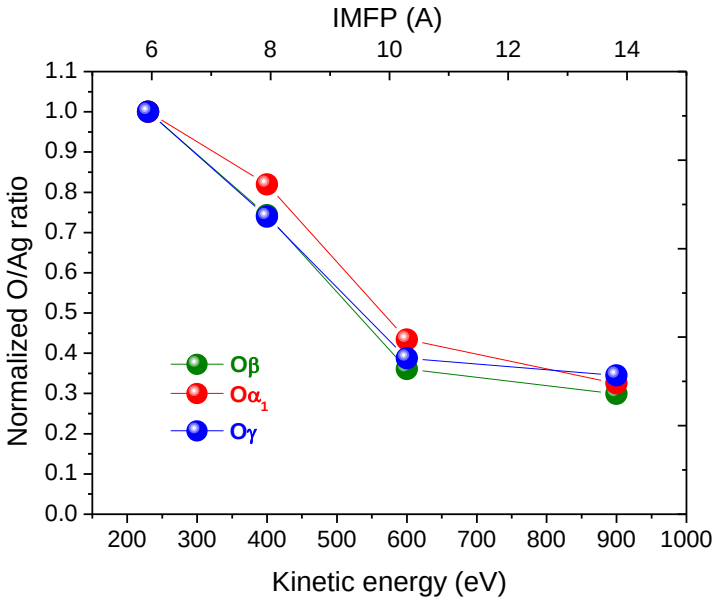


Figure S8: Normalized atomic O/Ag ratio as function of the photoelectron kinetic energy

Elemental depth distribution by energy dependent XPS was already performed in the same instrument for different systems (ref S2). The lack of depth information in the case of the Ag-O system seems to lie in the strong surface roughening of the Ag surface in the presence of O at elevated temperatures. Ag roughening due to surface restructuring in the presence of oxygen was already extensively investigated in the literature and our SEM images confirm the presence of roughening.

In order to get more insights about the depth distribution of different O species, simple numeric calculation of the expected O/Ag ratio for different coverage and depth distributions have been performed. Assuming that only inelastic scattering occurs with a probability $P(z) = (1/\lambda)\ e^{-(z/\lambda\cos\theta)}\ dz$ where $\lambda$ is the inelastic mean free path and $\theta$ is the emission angle (angle of the analyser axis with the microscopic local surface normal). The escape depth probability, i.e the probability of traveling a depth "d" without suffering inelastic scattering is given by

$$1-\frac{1}{\lambda}\int_0^d e^{-\frac{z}{\lambda}}dz = e^{-\frac{d}{\lambda\cos\theta}}$$

The next step is to assume a structural model, in this case, the Ag(111) with Ag atomic layers separated by 2.36 A and O atoms substituting Ag atoms. Finally, one more approximation is made by assuming that photoelectrons are not scattered by the oxygen atoms, so the Ag IMFP is used. Then the expected O/Ag ratio for each kinetic energy in a depth profile experiment can be numerically calculated by:

$$\frac{O}{Ag} = \frac{\sum_{layers} N_i(O).e^{-\frac{di}{\lambda(KE)\cos\theta}}}{\sum_{layers} N_i(Ag).e^{-\frac{di}{\lambda(KE)\cos\theta}}}.$$

Where Ni(X) is the layer occupation number ranging from 1 (full monolayer) to 0, which defines the coverage and depth distribution of oxygen atoms, $d_i$ is the distance of the layer to the surface, $\lambda$(KE) is the IMFP for each kinetic energy taken from ref S1 and the sum is extended to many layers until the calculated O/Ag ratio changes by less than 0.1%.

Table S4 presents an example for the case of the Ag(1111)-Op(4x4) reconstruction which has a surface coverage of 0.33 ML (obtained by geometrical construction) with normal emission. Calculations of depth profiles for different coverage of the O overlayer at similar kinetic energies experimentally measured are presented in figure S8. First, the case of oxygen overlayer on flat Ag surfaces at normal emission ($\theta$ = 0) with different coverage is presented in figure S9-a. All the curves show identical exponential decay, dropping to 50% of the initial O/Ag value from 200 to 900 eV. The depth profile curves for different O depth distributions (figure S9-c) are presented in figure S9-d. As can be seen, the presence of subsurface oxygen changes the shape of the normalized O/Ag ratio and reduces its slope. In order to evaluate the influence of roughening, the emission angle was averaged (0-90) and the obtained normalized O/Ag ratio is presented in figure S8-b together with the case of normal emission. As can be seen, the influence of roughening is very similar to presence of subsurface oxygen.

Table S4 – example of O/Ag ratio calculation for the case of overlayer oxygen with 33% coverage and 230 eV kinetic energy photoelectrons

| layer | Distance (A) | Ag Occupation | O Occupation (ML) | Escape probability exp(-d/l) |
|---|---|---|---|---|
| **over** | - | 0 | 0.33 | 1 |
| **1st** | 0 | 1 | 0 | 1 |
| **2nd** | 2.36 | 1 | 0 | 0.67 |
| **3rd** | 4.72 | 1 | 0 | 0.46 |
| **4th** | 7.08 | 1 | 0 | 0.31 |

208

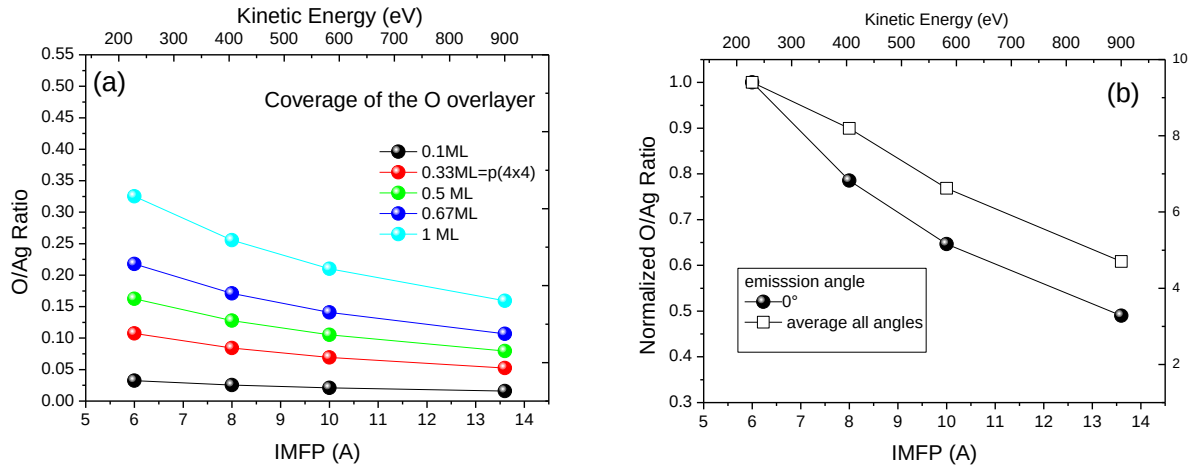


209

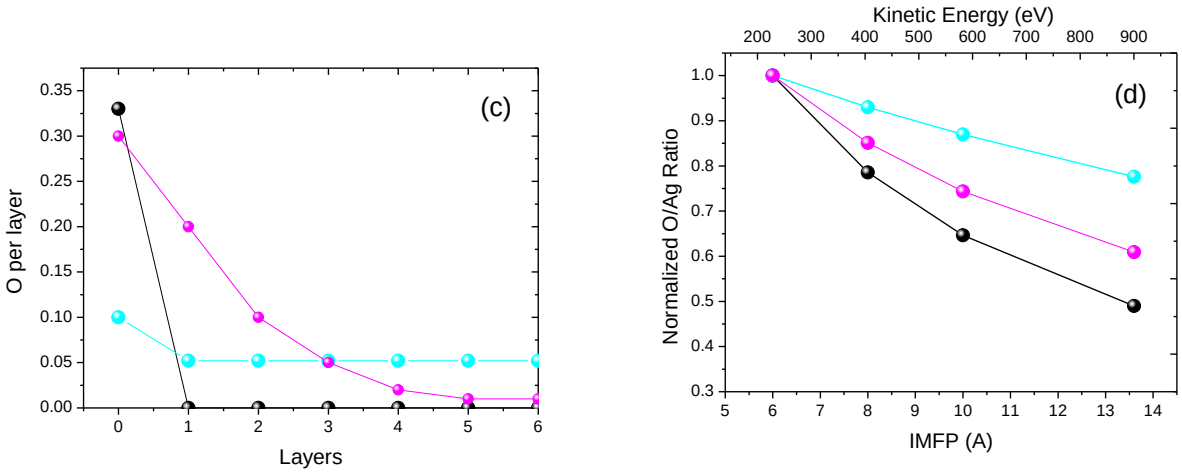


210

211 Figure S9. Numerically calculated O/Ag ratio as function of the photoelectron kinetic energy. (a) O
212 overlayer on Ag at different coverages with normal emission. (b) comparison of normalized O/Ag ratio
213 for normal emission and angle averaged. (c) depth distribution profiles for O on Ag. (d) respective
214 normalized O/Ag ratio obtained for the depth distribution presented in (c).